Biochimica et Biophysica Acta 1827 (2013) 38–49

Contents lists available at SciVerse ScienceDirect

Biochimica et Biophysica Acta

journal homepage: www.elsevier.com/locate/bbabio

Sirtuin-4 modulates sensitivity to induction of the mitochondrial permeability transition pore

Manish Verma, Nataly Shulga, John G. Pastorino *

Department of Molecular Biology, School of Osteopathic Medicine, University of Medicine and Dentistry of New Jersey, Stratford, NJ 08084, USA

ARTICLE INFO

Article history:
Received 3 May 2012
Received in revised form 14 September 2012
Accepted 23 September 2012
Available online 5 October 2012

Keywords:
Sirtuin-4
Mitochondria
Permeability transition pore
Oxidative stress

ABSTRACT

The sustained opening of the mitochondrial permeability transition pore (PTP) is a decisive event in the onset of irreversible cell injury. The PTP is modulated by numerous exogenous and endogenous effectors, including mitochondrial membrane potential, ions and metabolites. Mitochondrial sirtuins have recently emerged as pivotal mediators of mitochondrial metabolism. In the present study, we demonstrate that sirt-4 modulates sensitivity to PTP onset induced by calcium and the oxidative cross linking reagent phenylarsine oxide, and PTP dependent cytotoxicity brought about by TNF or doxorubicin. Moreover, the ability of sirt-4 to modulate onset of the PTP is dependent on the expression of glutamate dehydrogenase-1.

1. Introduction

Opening of the mitochondrial permeability transition pore (PTP) is a critical juncture in the evolution of mitochondrial injury and onset of necrotic cell death incited by a number of conditions, one prominently being oxidative stress caused by ischemia/reperfusion [1–3]. Despite significant efforts, the constituents of the PTP remain remarkably elusive. However, progress has been made in identifying endogenous regulators of PTP sensitivity, the most critical being cyclophilin-D [4,5]. Exogenous factors such as oxidative stress and calcium overload were identified early on as being capable of increasing sensitivity to PTP opening [6–8]. In particular, the thiol reactive agent, phenylarsine oxide (PAO), served as a useful tool to study the effects of oxidative modification of mitochondrial constituents on PTP sensitivity [9,10]. Induction of PTP opening by PAO is dependent on cyclophilin-D and is sensitive to inhibition of cyclophilin-D peptidyl-prolyl cis-trans isomerase activity by agents such as cyclosporin A.

Recently, mitochondrial sirtuins have emerged as critical regulators of mitochondrial metabolism, controlling metabolic processes such as mitochondrial fatty acid oxidation and urea synthesis [11,12]. We have shown that sirtuin-3 mediates the deacetylation of cyclophilin-D, and in so doing inhibits its peptidyl-prolyl cis-trans isomerase activity [13]. Inhibition or down-regulation of sirtuin-3 increases cyclophilin-D acetylation and activity, which in turn sensitizes mitochondria to PTP opening. Sirtuin-4, also localized to the mitochondria, lacks deacetylase activity, but possesses ADP-ribosyltransferase activity [14,15]. In the present report, we show that in contrast to sirt-3, down-regulation of sirtuin-4 expression renders mitochondria resistant to PTP induction. Moreover, the resistance to PTP induction exerted by suppression of sirt-4 is dependent on glutamate dehydrogenase-1 (GDH-1). GDH-1 is localized to the mitochondrial matrix and is negatively regulated by sirt-4. Depletion of GDH-1 negates the protection against PTP induction afforded by sirt-4 down-regulation, while stimulation of GDH-1 by leucine prevents PTP induction. Moreover, suppression of sirt-4 expression protects against PTP dependent cytotoxicity induced by TNF and doxorubicin.

2. Materials and methods

2.1. Cell culture and treatment

HeLa cells (American Type Culture Collection) were maintained in 25 cm^2 flasks (Corning Costar, Corning, NY) with 5 ml Dulbecco's modified Eagle's medium containing 100 U/ml penicillin, 0.1 mg/ml streptomycin and 10% heat-inactivated fetal bovine serum and incubated at 37 °C under an atmosphere of 95% air and 5% CO_2.

For time lapse fluorescent microscopy, cells were plated in Labtek® 8 well chamber slides™ (Nunc, Rochester, NY) at 25,000 cells/well in DMEM containing glucose at 4.5 g/l. Treatments with cyclosporin A (10 μM) or leucine (1 mM) were done for 5 minutes before start of image acquisition.

2.2. Reagents

TransIT-TKO® transfection reagent was purchased from Mirus (Madison, WI). Phenylarsine oxide and carbonyl cyanide

* Corresponding author at: University of Medicine and Dentistry of New Jersey, Department of Molecular Biology, Science Center, Room 316, Stratford, NJ 08084, USA. Tel.: +1 856 566 6041; fax: +1 856 566 6291.
E-mail address: pastorjg@umdnj.edu (J.G. Pastorino).

0005-2728/$ – see front matter © 2012 Elsevier B.V. All rights reserved.
http://dx.doi.org/10.1016/j.bbabio.2012.09.016

3-chlorophenylhydrazone are from Sigma. Cyclosporin A was from Biomol Research Laboratories. Digitonin was from Calbiochem. Tetramethylrhodamine Methyl Ester Perchlorate (TMRM) was from Molecular Probes (Life technologies).

2.3. siRNA mediated knockdown of sirtuin-4, sirtuin-3, sirtuin-5, cyclophilin-D and GDH-1

A lipid based method (Mirus, Madison, WI) was used to deliver siRNAs targeting sirtuin-4, glutamate dehydrogenase-1 (GDH-1), sirt-3, sirt-5, cyclophilin-D (CyP-D) or a non-targeting control into HeLa cells. The final concentration of the siRNAs was 50 nM. The siRNA–liposome complexes were added to the cells for 24 hours, after which the cells were washed two times with phosphate buffered saline and fresh complete DMEM was added. The cells were incubated for another 24 hours and then utilized for experiments.

2.4. Time lapse fluorescence microscopy

Prior to image acquisition, HeLa cells were loaded with 200 nM TMRM or 200 nM of MitoSOX for 30 minutes. Cells were then washed two times with wash buffer (50 mM Tris, 1 mM EGTA, pH 7.5). After a second wash, cells were placed in respiratory medium (0.5 mM EGTA, 3 mM $MgCl_2$, 60 mM potassium lactobionate, 20 mM taurine, 10 mM KH_2PO_4, 20 mM HEPES, 110 mM sucrose, 1 g/l BSA, 2 μM oligomycin and 1 mM of succinate as the respiratory substrate) on a heated stage maintained at 37 °C. After initial loading, 20 nM of TMRM or 20 nM of MitoSOX were also present in the respiratory medium to prevent their redistribution. Digitonin at 2.5 μg/ml was added to selectively permeabilize the plasma membrane. After a five minute pre-incubation, images were taken at 1 minute intervals for 20 minutes with an Olympus IX 51 microscope at 20X magnification. Where indicated, phenylarsine oxide or calcium were added after 2 minutes and CCCP was added after 18 minutes to induce complete depolarization. For determination of ROS production with MitoSOX, the experiments were conducted as with TMRM. HeLa cells were loaded with 5 μM of MitoSOX for 30 minutes. Treatment and image acquisition were identical to TMRM.

Images were analyzed using Slidebook (Intelligent Imaging Innovations, Denver, CO) software. Region of interests were drawn around the cells, pixel intensity was measured and averaged for each image. The dynamics of TMRM fluorescence was calculated by the following formula (Observed Intensity − Final Image Intensity)/(First Image Intensity − Final Image Intensity)*100. The data were then imported into Sigma Plot and utilized to generate line graphs for each condition. To provide more clarity to the graphs, a constant was added or subtracted from the data sets of each condition to prevent the traces from overlapping. The mean of the data obtained from three separate experiments was then used to generate the line graphs presented in Figs. 1, 2, 4 and 5. For MitoSOX, intensity measurements were done similarly to TMRM experiments. Increases in fluorescence intensity at one minute intervals were compared to the intensity of the first image at the zero minute time point and represented in % by using the formula: % change in MitoSOX fluorescence intensity = (observed image intensity − first image intensity)/(first image intensity)*100. A bar graph was made using the time points at 3 and 20 minutes. The results presented are the mean of three independent experiments with error bars indicating standard deviation.

2.5. Measurement of cell viability

Following treatments, L929 or HeLa cells were harvested and centrifuged at 700*g*. The cell pellet was re-suspended in phosphate buffered saline to which was added 5 μM of propidium iodide. After 5 minutes incubation, the cells were pelleted and re-suspended in PBS. The percentage of viable cells was determined utilizing a Cellometer (Nexelom) as the ratio of the number of cells in the fluorescent images (propidium iodide positive) to the bright field images.

2.6. Micoplate assay for mitochondrial depolarization and H_2O_2 production

HeLa cells were plated at 50,000 cells/well in 24 well plates and transfected with the indicated siRNAs. After 48 hours, the cells were loaded with 200 nM TMRM in DMEM for 30 minutes. After loading, the cells were washed once with wash buffer. After washing, cells were incubated further for 5 minutes in respiratory buffer containing 2.5 μg/ml digitonin and 20 nM of TMRM. Fluorescence intensity was measured using a Synergy HT microplate reader with an excitation of 550 nm and emission at 573 nm at 37 °C for 30 second intervals. After 4 minutes, either phenylarsine oxide or Ca^{2+} was added at the indicated concentration, with fluorescence measured over 20 minutes. For complete depolarization 2.5 μM of CCCP was added after 4 minutes. The results are presented as % of TMRM retained in non-treated cells transfected with non target siRNA at the 20 minute time point. For the Amplex red assay, HeLa cells were plated and then transfected with siRNAs targeting sirt-4, and CyP-D either individually or in tandem with siRNA targeting GDH-1. Following 48 hours, the cells were placed in respiratory buffer and permeabilized with digitonin (2.5 μg/ml). Amplex-red reagent was added at 5 μM along with 10 U/ml of horseradish peroxidase. Following addition of Ca^{2+} or PAO, fluorescence intensity was measured using Synergy HT microplate reader with an excitation of 570 nm and emission at 585 nm at 37 °C at 1 minute intervals.

2.7. Isolation of mitochondria

Following treatments, approximately 400,000 cells total obtained from 4 wells of a 24 well plate were harvested by trypsinization and centrifuged at 700*g* for 10 minutes at 4 °C. The cell pellets were washed once in PBS and then resuspended in 3 volumes of isolation buffer (20 mM Hepes, pH 7.4, 10 mM KCl, 1.5 mM $MgCl_2$, 1 mM sodium EDTA, 1 mM dithiothreitol, 10 mM phenylmethylsulfonyl fluoride, 10 μM leupeptin and 10 μM aprotinin) in 250 mM sucrose. After chilling on ice for 3 minutes, the cells were disrupted by 40 strokes of a glass homogenizer. The homogenate was centrifuged twice at 1500*g* at 4 °C to remove unbroken cells and nuclei. The mitochondria-enriched fraction was then pelleted by centrifugation at 12,000*g* for 30 minutes.

2.8. Measurement of glutamate dehydrogenase-1 activity

Glutamate dehydrogenase (GDH-1) activity in HeLa cells was measured using the GDH activity assay kit from BioVision (Mountain View, CA). Briefly, 50,000 cells/well were plated in 24 well plates. Transfection was carried out as described above. Forty eight hours after transfection, cells from four wells were harvested by trypsinization and washed twice with ice cold PBS. Mitochondria were isolated and lysates prepared. Optical density at 450 nm was measured with a Synergy HT microplate reader (BioTek, Winooski, VT) at 37 °C at 3 minute intervals for 1 hour. The results are expressed as the percentage increase or decrease in activity compared to non-treated cells transfected with non-targeting control siRNA.

2.9. Measurement of mitochondrial glutathione

Glutathione (GSH) was estimated using a monobromobimane fluorochrome based assay according to the manufactures instruction (Millipore, Billerica, MA). Briefly, 50,000 cells/well were plated in 24 well plate. Transfection was carried out as described above. Forty eight hours after transfection, cells from four wells were harvested by trypsinization and washed twice with ice cold PBS. All procedures were done on ice and as rapidly as possible to prevent GSH oxidation. Mitochondria were isolated and lysates prepared. The supernatant

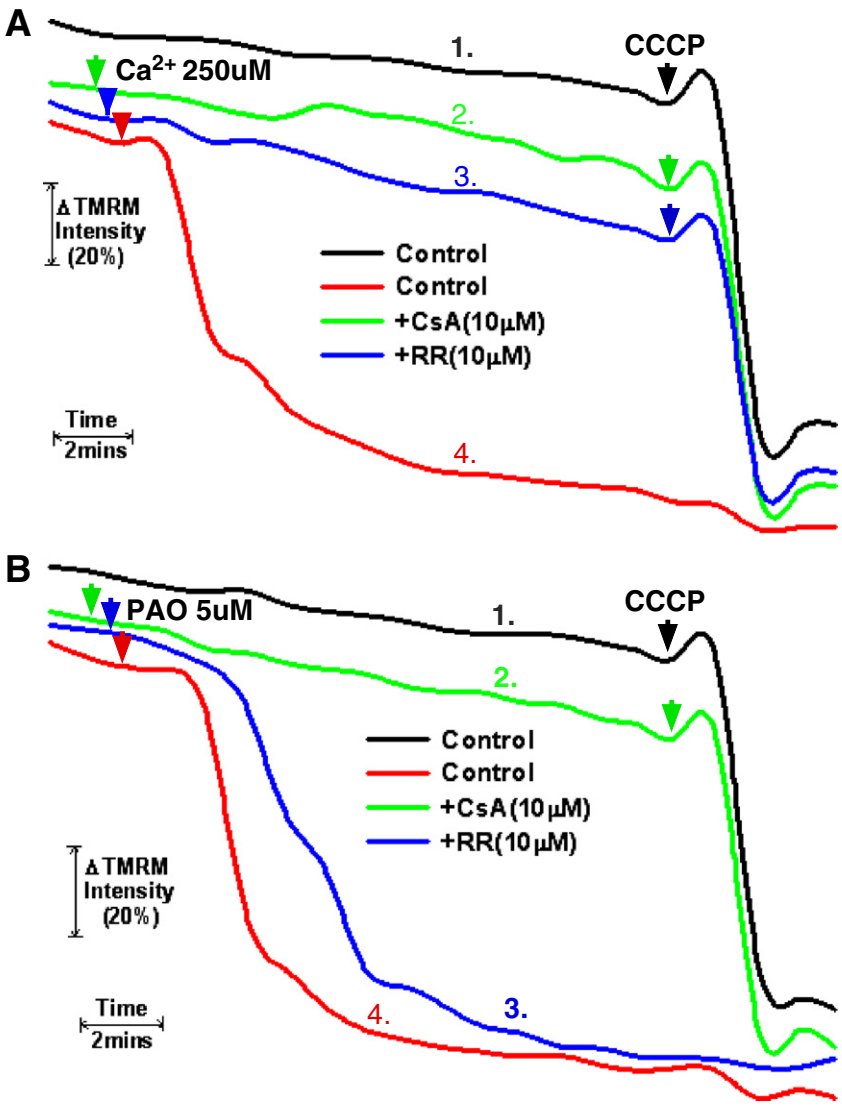

Fig. 1. Measurement and control of PTP induction in permeabilized cells. A and B. HeLa cells were loaded with 200 nM TMRM in DMEM for 30 minutes. The cells were then washed twice with PBS and incubated further for 5 minutes in respiratory buffer containing 20 nM of TMRM. Digitonin at 2.5 μg/ml was then added to permeabilize the plasma membrane and the cells were mounted on a heated stage kept at 37 °C. Where indicated, cells were pretreated with 10 μM of cyclosporin A or ruthenium red for 5 minutes. Phenylarsine oxide (PAO) or Ca^{2+} was added at final concentrations of 5 μM and 250 μM, respectively. TMRM fluorescence was monitored over a 20 minute time course. 5 μM of CCCP was added at the 18 minute time point. The result is the average of three independent experiments.

was used to determine the GSH content. Fluorescence was measured at excitation of 308 nm and emission of 460 nm using Synergy HT microplate reader. The results are presented as percentage of GSH content compared to non-treated and non target transfected cells.

2.10. Measurement of mitochondrial Ca^{2+} retention capacity

The Ca^{2+} retention capacity was measured fluorimetrically on a microplate reader at 37 °C in the presence of the Ca^{2+} indicator Calcium Green-5N (1 μM; excitation: 505 nm; emission: 535 nm; Molecular Probes). Whole cells were placed in respiratory buffer containing 1 mM succinate and permeabilized with digitonin. Calcium was added in pulses of 10 μM and uptake measured as a decrease of Calcium Green-5N fluorescence. Calcium was added in pulses until onset of the PTP occurred as indicated by a rapid rise of calcium-green-5 N fluorescence. To allow calculation of medium Ca^{2+} from the measured fluorescence values, each experiment was ended by the addition of 10 μM of the uncoupler carbonylcyanide 3-chlorophenylhydrazone (CCCP) followed by 400 μM EGTA, to be in excess of total Ca^{2+} added during the study to determine the minimum fluorescence intensity (F_{min}) value, followed by 4 mM $CaCl_2$ to determine the maximum fluorescence intensity (F_{max}) value. The results are average of three independent experiments.

2.11. Statistical analysis

Results are expressed as means ± s.d. of at least three independent experiments. Statistical significance was defined at $P<0.05$.

3. Results

3.1. Determination of mitochondrial permeability transition in permeabilized cells

As shown in Fig. 1A, trace #1, as measured by TMRM fluorescence, HeLa cells permeabilized with digitonin maintain a relatively stable mitochondrial membrane potential. Significantly, addition of the mitochondrial un-coupler, CCCP, at 18 minutes caused a rapid decline of TMRM fluorescence, indicating depolarization of the mitochondria.

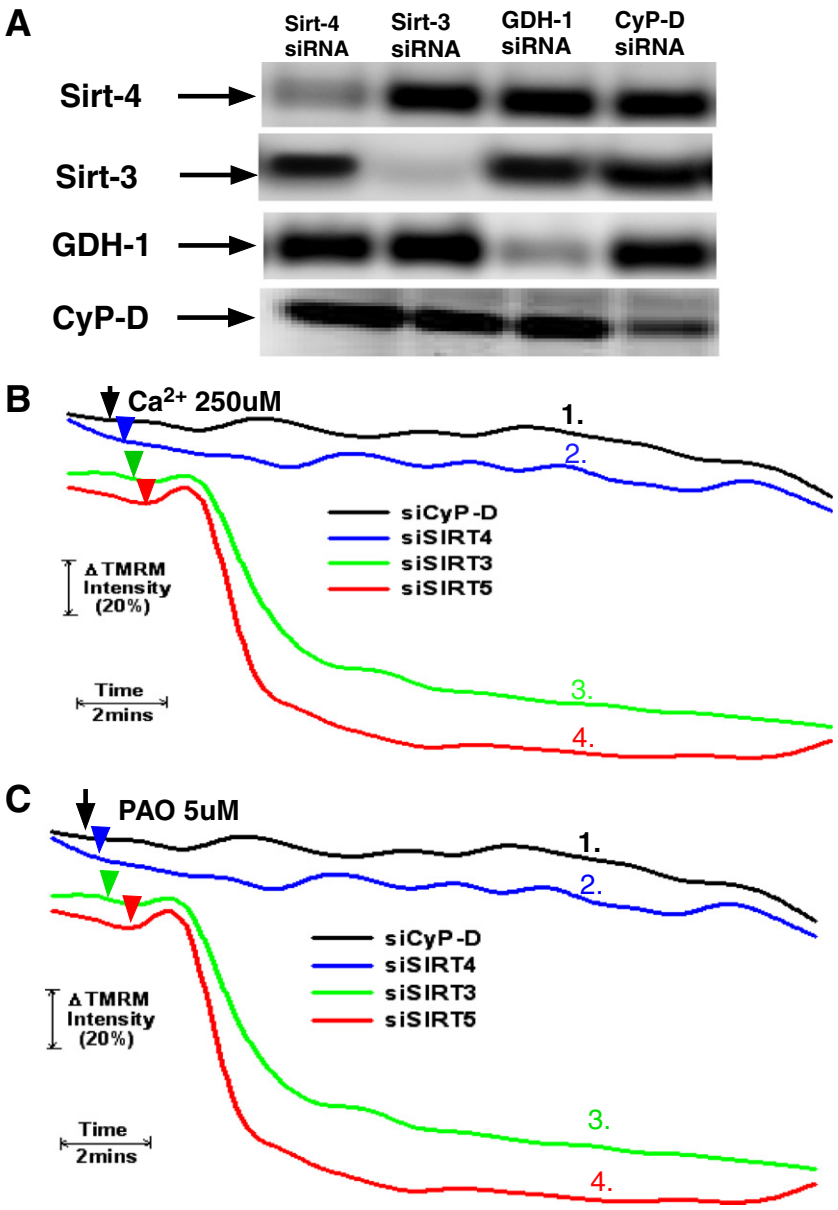

Fig. 2. Sirt-4 controls sensitivity to PTP induction by Ca^{2+} and PAO. A. HeLa cells were plated and then transfected with siRNAs targeting sirt-4, sirt-3, sirt-5, cyclophilin-D or a non-targeting control. Following 48 hours, the cells were harvested. Mitochondrial extracts were prepared and separated on 12% SDS-PAGE gels followed by blotting to PVDF membranes. The western blots were developed with antibodies against sirt-4, CyP-D, GDH-1, sirt-3 or sirt-5. The results are representative of three independent experiments. B and C. HeLa cells were plated and then transfected with siRNAs targeting sirt-4, sirt-3, sirt-5 or cyclophilin-D. Following 48 hours, the cells were loaded with 200 nM TMRM in DMEM for 30 minutes. The cells were then washed twice with PBS and incubated further for 5 minutes in respiratory buffer containing 20 nM of TMRM. Digitonin at 2.5 μg/ml was then added to permeabilize the plasma membrane and the cells were mounted on a heated stage kept at 37 °C. the cells were loaded with TMRM and mounted on a heated microscopy stage. Following permeabilization with digitonin, Ca^{2+} or PAO were added at final concentrations of 250 μM and 5 μM, respectively. Time-lapse microscopy was conducted over a 20 minute time course with TMRM fluorescence intensity assessed as described in Materials and methods. The result is the average of three independent experiments.

Addition of calcium (Ca^{2+}) to give a final free calcium concentration of 250 μM also provoked mitochondrial depolarization (Fig. 1A, trace #4). Significantly, the depolarization brought about by Ca^{2+} was due to sustained opening of the permeability transition pore (PTP). Cyclophilin-D is a critical mediator of PTP sensitivity, with cyclosporin A (CsA) inhibiting the peptidyl-prolyl cis-trans isomerase activity of cyclophilin-D and lessening sensitivity to PTP induction. A five minute pretreatment with 10 μM of CsA completely prevented the calcium induced mitochondrial depolarization, but had no effect on loss of TMRM fluorescence upon subsequent addition of CCCP (Fig. 1A, trace #2). Significantly, inhibition of the calcium uniporter with ruthenium-red, which inhibits mitochondrial calcium uptake, also prevented induction of the PTP brought about by calcium (Fig. 1A, trace #3).

Phenylarsine oxide (PAO) induces PTP opening independently of an increase of Ca^{2+} by an oxidative dependent cross-linking of PTP components. As shown in Fig. 1B, trace #4, addition of 5 μM PAO induced rapid mitochondrial depolarization, which was prevented by pre-treatment with CsA (Fig. 1B, trace #2). As would be expected, ruthenium-red had no effect on the ability of PAO to induce the PTP, since in this instance, PTP induction is calcium independent (Fig. 1B, trace #3). These results confirm that the permeabilized cell system

recapitulates the behavior of isolated mitochondria with regards to agents capable of inducing and inhibiting the PTP.

3.2. Suppression of sirtuin-4 prevents Ca^{2+} and PAO induction of the PTP

HeLa cells were transfected with siRNAs targeting sirtuin-4, sirtuin-3, glutamate dehydrogenase I (GDH-1) or CyP-D (cyclophilin-D). As shown in Fig. 2A, the siRNAs selectively suppressed the expression of their targets while having minimal off-target effects. The siRNA targeting sirt-4 suppressed its expression by 85% ± 6% by densitometry analysis. Particularly important is that the siRNA targeting sirt-4 had no effect on the expression of cyclophilin-D. Similarly, GDH-1 and CyP-D suppressed the expression of their respective targets by 89% ± 7%and 79% ± 5%, respectively. As shown in Fig. 2B and C (trace #1), depletion of cyclophilin-D (CyP-D) prevented PTP induction by both Ca^{2+} and PAO, respectively. Remarkably, as shown in Fig. 2B, trace #2, cells in which sirt-4 was depleted exhibited robust resistance to PTP induction brought about by the addition of Ca^{2+}. Similarly, depletion of sirtuin-4 rendered mitochondria resistant to PTP induction by PAO to the same degree as CyP-D knock-down (Fig. 2C, trace #2). Importantly, suppression of sirt-3 or sirt-5, both localized to the mitochondria, did not prevent PTP induction by either Ca^{2+} or PAO (Fig. 2B and C, traces #3 and #4, respectively).

Induction of the PTP is frequently accompanied by an increased generation of reactive oxygen species (ROS) by mitochondria. The fluorescent probe, MitoSOX, localizes to the mitochondria and exhibits increased fluorescence upon stimulation of mitochondrial superoxide anion production. As shown in Fig. 3A, addition of 1 mM of H_2O_2 brought about a 57% increase of MitoSOX fluorescence over a twenty minute time course, indicating the ability of MitoSOX to detect ROS in the permeabilized cell system. Importantly, induction of the PTP by Ca^{2+} or PAO was accompanied by generation of ROS. Exposure to 250 μM of Ca^{2+} or 5 μM of PAO induced a 43–46% stimulation of ROS generation in cells transfected with non-targeting siRNA (Fig. 3A and B, respectively). The generation of ROS by Ca^{2+} or PAO was due to PTP induction, as both were prevented by either suppressing cyclophilin-D expression or pretreatment with CsA (Fig. 3A and B). Importantly, as with mitochondrial depolarization, depletion of sirt-4 prevented ROS production induced by both Ca^{2+} and PAO to the same degree as depletion of cyclophilin-D or pre-treatment with CsA (Fig. 3A and B).

Mitochondria produce superoxide anion, which is converted to H_2O_2 by mitochondrial superoxide anion dismutase. Utilizing the Amplex-Red assay, we determined the rate of H_2O_2 production. As shown in Fig. 3C, the addition of 250 μM of Ca^{2+} or 5 μM of PAO to permeabilized Hela cells resulted in an over 5 fold increase in the rate of H_2O_2 production. Importantly, suppression of CyP-D expression inhibited H_2O_2 production brought about by Ca^{2+} or PAO as did depletion of sirt-4, suggesting that both prevent H_2O_2 production by inhibiting onset of the PTP.

3.3. Modulation of the PTP by sirt-4 is dependent on glutamate dehydrogenase-1

Sirt-4 ADP ribosylates and inactivates glutamate dehydrogenase-1 (GDH-1); therefore the protective effect of depleting sirt-4 against PTP induction maybe due to activation of GDH-1. If this is the case, then suppression of GDH-1 expression should restore PTP sensitivity when sirt-4 levels are depleted. Therefore HeLa cells were concomitantly transfected with siRNAs targeting sirt-4 and GDH-1. As show in Fig. 4A and B, traces #2, depletion of GDH-1 reversed the protective effect exerted by suppressing sirt-4 expression on PTP induction brought about by either Ca^{2+} or PAO, respectively. Importantly, depletion of GDH-1 did not reverse the inhibition of PTP induction mediated by suppression of CyP-D, indicating that GDH-1 acts specifically in a sirt-4 dependent pathway to modulate PTP sensitivity (Fig. 4A and B, traces #1). Additionally, the prevention of ROS production by down-regulation of sirt-4 was also dependent on GDH-1 expression. As shown in Fig. 4C and D, depletion of GDH-1 prevented down-regulation of sirt-4 from inhibiting Ca^{2+} or PAO induced ROS generation, with the addition of Ca^{2+} or PAO triggering a 45%–58% increase in ROS production in cells where sirt-4 and GDH-1 were concomitantly down-regulated, respectively. By contrast, depletion of GDH-1 expression did not reverse the ability of CyP-D suppression to prevent Ca^{2+} or PAO induced ROS production, with only a 10–12% stimulation of ROS production when CyP-D and GDH-1 were concomitantly down-regulated, indicating that unlike sirt-4, CyP-D modulation of PTP induced ROS production is not dependent on GDH-1 expression (Fig. 4C and D). Similarly, the ability of sirt-4 depletion to prevent an increased rate of H_2O_2 production was dependent on the expression of GDH-1. As shown in Fig. 4E, suppression of GDH-1 expression reversed the protective effect of sirt-4 depletion against Ca^{2+} and PAO stimulation of H_2O_2 production. By contrast, the ability of CyP-D depletion to prevent onset of H_2O_2 production by Ca^{2+} or PAO was not dependent on GDH-1.

In addition to reversing the protective effect against PTP induction exerted by sirt-4 depletion, suppression of GDH-1 potentiated PTP induction triggered by sub-threshold doses of Ca^{2+} and PAO. As shown in Fig. 5A, trace #1, in cells transfected with a non-targeting siRNA, a 50 μM dose of Ca^{2+} induced the PTP to a much lesser extent than a 250 μM dose, exhibiting a longer lag phase to PTP induction and incomplete depolarization over a twenty minute time course, indicating that a large proportion of the mitochondria were resistant to PTP induction by this low dose of Ca^{2+}. By contrast, when GDH-1 levels were depleted, 50 μM of Ca^{2+} induced rapid and complete PTP induction, comparable in rapidity and extent to that induced by a 250 μM dose of Ca^{2+} in control cells (Fig. 5A, trace #2). Similarly, a sub-threshold dose of PAO (2.5 μM) that induced incomplete depolarization in cells transfected with non-target siRNA (Fig. 5B, trace #1), induced rapid and complete loss of membrane potential in cells where GDH-1 levels are depleted (Fig. 5B, trace #2).

Leucine is an allosteric stimulator of GDH-1 [16,17]. As show in Fig. 5C, trace #2, in cells transfected with non-targeting siRNA, treatment with 250 μM Ca^{2+} induced rapid mitochondrial depolarization. By contrast, cells pretreated for 5 minutes with 1 mM of leucine were refractory to PTP induction brought about by the addition of 250 μM calcium (Fig. 5C, trace #1). Moreover, the ability of leucine to prevent PTP induction was dependent on expression of GDH-1. As shown in Fig. 5C, trace #3, depletion of GDH-1 neutralized the ability of leucine to prevent PTP induction by calcium, indicating that prevention of the PTP by leucine is dependent on GDH-1 expression. Similarly, exposure of cells transfected with non-targeting siRNA to 5 μM of PAO brought about rapid mitochondrial depolarization that was prevented by pretreatment with 1 mM of leucine (Fig. 5D, traces #2 and #1, respectively). However as with Ca^{2+}, the ability of leucine to prevent induction of the PTP by PAO was dependent on GDH-1, with depletion of GDH-1 reversing the protective effect of leucine (Fig. 5D, trace #3). These data indicate that GDH-1 increases the threshold for PTP induction and that when the negative regulation exerted on GDH-1 by sirt-4 is removed, PTP induction is blunted.

In order to verify the results obtained utilizing fluorescence microscopy, a plate reader assay was employed to determine the ability of digitonin permeabilized cells to retain TMRM upon a challenge with Ca^{2+} or PAO. As shown in Fig. 5E, in agreement with the results obtained with fluorescence microscopy, the addition of 250 μM of Ca^{2+} to digitonin permeabilized cells transfected with non-targeting siRNA resulted in a 93% loss of TMRM fluorescence. By contrast, cells pre-treated with CsA or depleted of CyP-D were resistant to calcium induced loss of TMRM fluorescence, exhibiting only a 10%–15% loss of TMRM fluorescence, indicating that the mitochondrial depolarization is due to opening of the PTP. Similarly, the addition of 5 μM of PAO brought about a 95% loss of TMRM fluorescence that was prevented by pre-treatment with

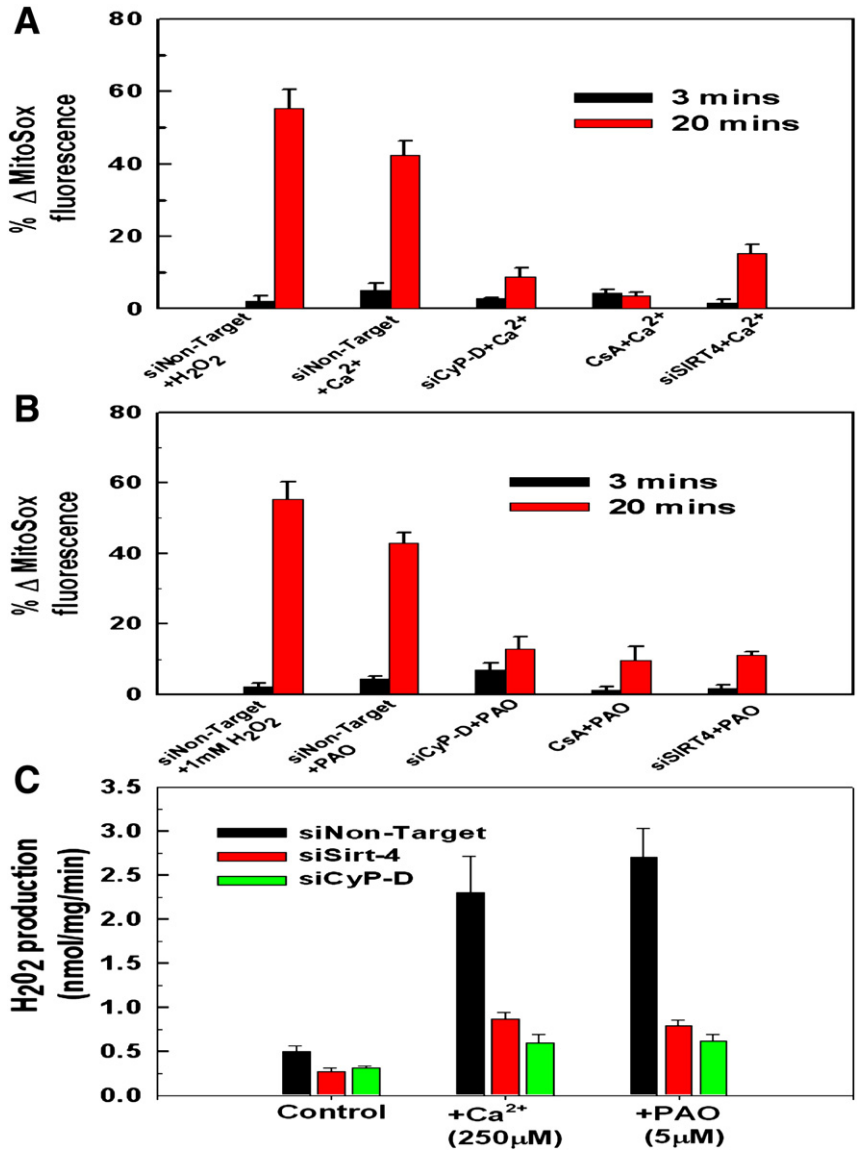

Fig. 3. Down-regulation of sirt-4 prevents PTP dependent ROS production. A and B. HeLa cells were plated and then transfected with siRNAs targeting sirt-4, cyclophilin-D or a non-targeting control. Following 48 hours the HeLa cells were loaded with 200 nM MitoSOX in DMEM for 30 minutes. The cells were then washed twice with PBS and incubated further for 5 minutes in respiratory buffer containing 20 nM of MitoSOX. Digitonin at 2.5 μg/ml was then added to permeabilize the plasma membrane and the cells were mounted on a heated stage kept at 37 °C. Where indicated, cells were pretreated with 10 μM of cyclosporin A for 5 minutes. Ca^{2+} and PAO were added at final concentrations of 250 μM and 5 μM, respectively. Time-lapse microscopy was conducted over a 20 minute time course with MitoSox fluorescence intensity assessed as described in Materials and methods. The results are the mean of three independent experiments ± the standard deviation. C. HeLa cells were plated and then transfected with siRNAs targeting sirt-4 or CyP-D. Following 48 hours, the cells were placed in respiratory buffer and permeabilized with digitonin (2.5 μg/ml). Amplex-red reagent was added at 5 μM along with 10 U/ml of horseradish peroxidase. Following addition of Ca^{2+} or PAO, fluorescence intensity was measured using a Synergy HT microplate reader with an excitation of 570 nm and emission at 585 nm at 37 °C at 1 minute intervals. The results are the mean of three independent experiments ± the standard deviation.

CsA or depletion of CyP-D. Importantly, depletion of sirt-4 also prevented Ca^{2+} and PAO induction of the PTP (Fig. 5E). In contrast to CsA or suppression of CyP-D expression, depletion of sirt-4 required the expression of GDH-1 to prevent PTP induction by Ca^{2+} or PAO (Fig. 5F). Suppression of GDH-1 expression reversed the protective effect exerted by depletion of sirt-4 against Ca^{2+} and PAO induced loss of TMRM fluorescence (green bar). Importantly, activation of GDH-1 by leucine also prevented induction of the PTP by Ca^{2+} and PAO, which was reversed by depletion of GDH-1 (Fig. 5F, yellow and blue bars, respectively). However, depletion of GDH-1 did not reverse the protective effect exerted by pretreatment with CsA or suppression of CyP-D expression on Ca^{2+} or PAO induction of the PTP, indicating that sirt-4 prevents the PTP via a GDH-1 dependent mechanism distinct from that mediated by inhibition of cyclophilin-D (Fig. 5F).

3.4. Sirt-4 increases mitochondrial calcium retention capacity

Desensitization to PTP opening increases the ability of mitochondria to take up calcium, thereby lessening cellular injury when calcium homeostasis is perturbed. Control, non-treated HeLa cells displayed a calcium retention capacity of 250 nmole of Ca^{2+}/mg mitochondrial protein. As shown in Fig. 6, as expected, treatment with CsA or suppression of CyP-D expression increased the ability of mitochondria to retain calcium by 87% and 93%, respectively. Importantly, depletion of sirt-4 enhanced calcium retention to the same degree,

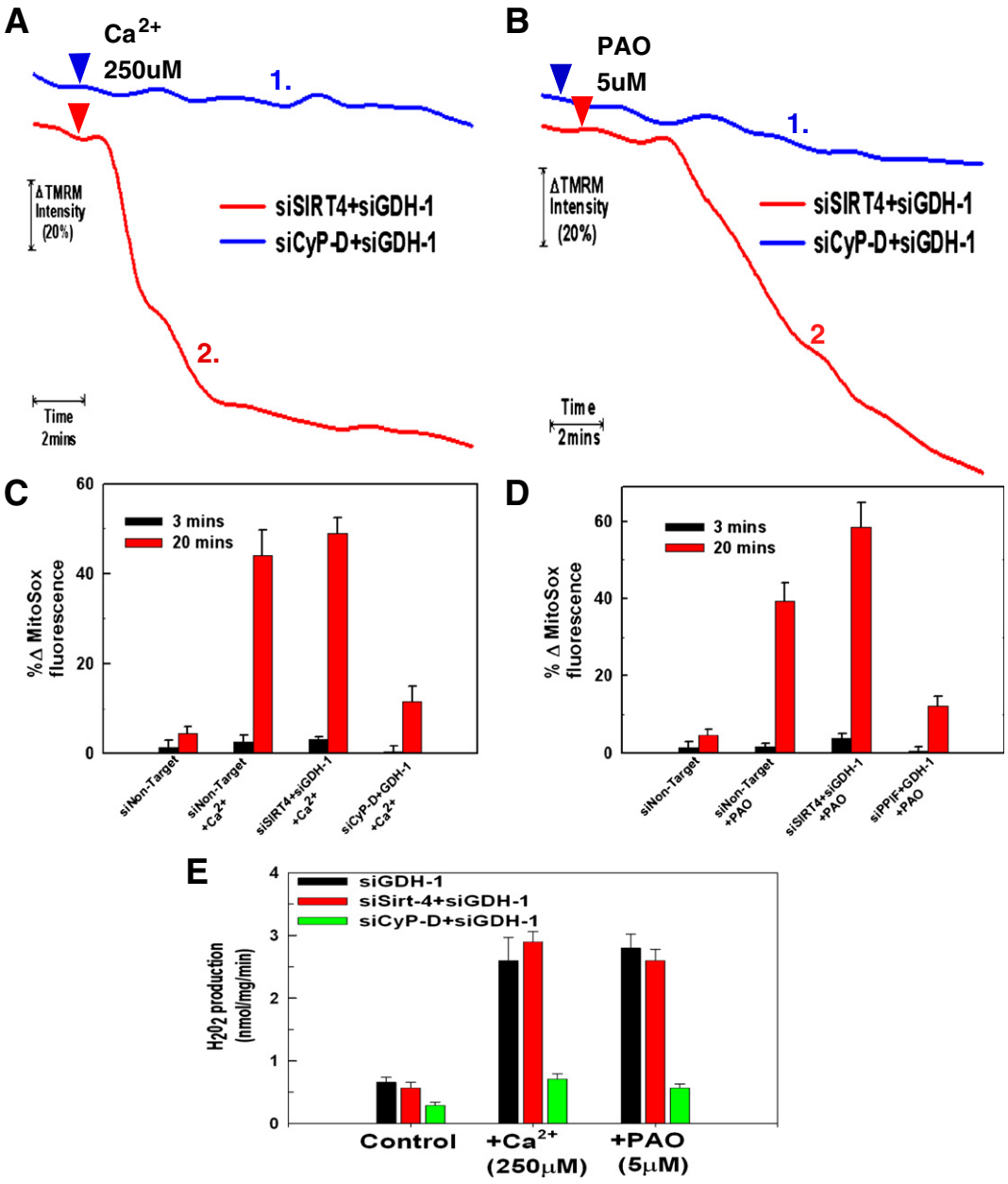

Fig. 4. Glutamate dehydrogenase-1 expression is necessary for sirt-4 depletion to protect against the PTP. A and B. HeLa cells were plated and then transfected with an siRNA targeting GDH-1 simultaneously with siRNAs targeting sirt-4 or cyclophilin-D. Following 48 hours, HeLa cells were loaded with 200 nM TMRM in DMEM for 30 minutes. The cells were then washed twice with PBS and incubated further for 5 minutes in respiratory buffer containing 20 nM of TMRM. Digitonin at 2.5 μg/ml was then added to permeabilize the plasma membrane and the cells were mounted on a heated stage kept at 37 °C. Following permeabilization with digitonin, Ca^{2+} and PAO were added at final concentrations of 250 μM and 5 μM, respectively. Time-lapse microscopy was conducted over a 20 minute time course with TMRM fluorescence intensity assessed as described in Materials and methods. The result is the average of three independent experiments. C and D. HeLa cells were plated and then transfected with an siRNA targeting GDH-1 simultaneously with siRNAs targeting sirt-4 or cyclophilin-D. Following 48 hours, the cells were loaded with 200 nM of MitoSOX in DMEM for 30 minutes. The cells were then washed twice with PBS and incubated further for 5 minutes in respiratory buffer containing 20 nM of MitoSOX. Digitonin at 2.5 μg/ml was then added to permeabilize the plasma membrane and the cells were mounted on a heated stage kept at 37 °C. Following permeabilization with digitonin, Ca^{2+} and PAO were added at final concentrations of 250 μM and 5 μM, respectively. Time-lapse microscopy was conducted over a 20 minute time course with MitoSOX fluorescence intensity assessed as described in Materials and methods. The results are the mean of three independent experiments ± the standard deviation. E. HeLa cells were plated and then transfected with siRNAs targeting sirt-4, CyP-D individually or in tandem with siRNA targeting GDH-1. Following 48 hours, the cells were placed in respiratory buffer and permeabilized with digitonin (2.5 μg/ml). Amplex-red reagent was added at 5 μM along with 10 U/ml of horseradish peroxidase. Following addition of Ca^{2+} or PAO, fluorescence intensity was measured using Synergy HT microplate reader with an excitation of 570 nm and emission at 585 nm at 37 °C at 1 minute intervals. The results are the mean of three independent experiments ± the standard deviation.

increasing capacity by 94%. Intriguingly, suppression of GDH-1 decreased calcium retention capacity to below control levels, in agreement with the notion that loss of GDH-1 expression potentiates induction of the PTP. Moreover, the ability of sirt-4 to increase calcium retention capacity is dependent on GDH-1 expression. Suppression of GDH-1 reversed the ability of sirt-4 depletion to enhance calcium retention capacity, depressing calcium retention capacity to levels below that of control. Similarly, stimulation of GDH-1 activity with leucine increased calcium retention capacity that in turn was reversed by depletion of GDH-1. By contrast, the ability of CsA to increase calcium retention capacity was not dependent on GDH-1 expression (Fig. 6).

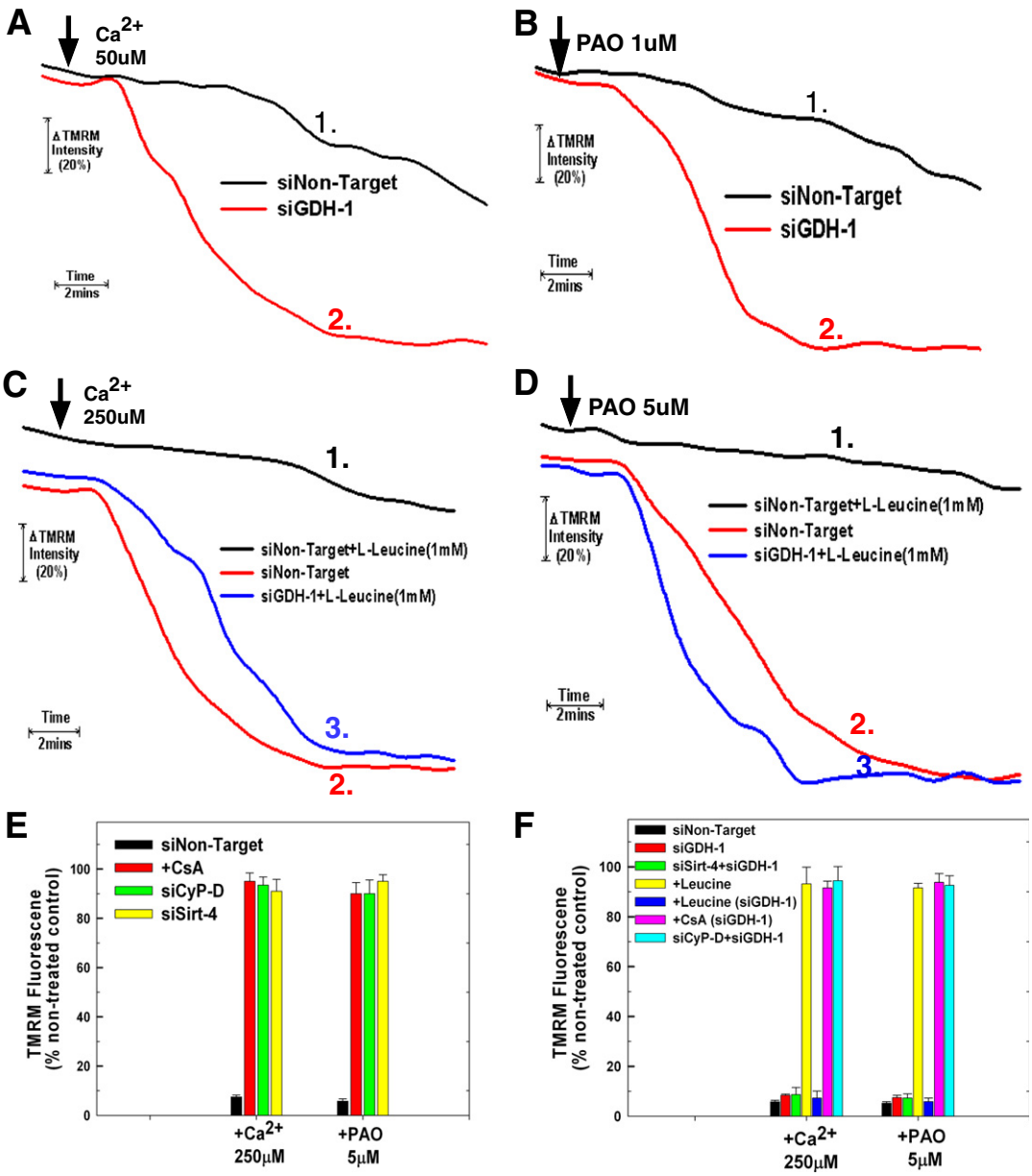

Fig. 5. Glutamate dehydrogenase regulates PTP sensitivity. A and B. HeLa cells were plated and then transfected with siRNAs targeting GDH-1 or a non-targeting control. Following 48 hours, HeLa cells were loaded with 200 nM TMRM in DMEM for 30 minutes. The cells were then washed twice with PBS and incubated further for 5 minutes in respiratory buffer containing 20 nM of TMRM. Digitonin at 2.5 μg/ml was then added to permeabilize the plasma membrane and the cells were mounted on a heated stage kept at 37 °C. Following permeabilization with digitonin, Ca^{2+} or PAO were added at final concentrations of 50 μM and 2.5 μM, respectively. Time-lapse microscopy was conducted over a 20 minute time course with TMRM fluorescence intensity assessed as described in Materials and methods. The result is the average of three independent experiments. C and D. HeLa cells were plated and then transfected with siRNAs targeting GDH-1 or a non-targeting control. Following 48 hours, HeLa cells were loaded with 200 nM TMRM in DMEM for 30 minutes. The cells were then washed twice with PBS and incubated further for 5 minutes in respiratory buffer containing 20 nM of TMRM. Digitonin at 2.5 μg/ml was then added to permeabilize the plasma membrane and the cells were mounted on a heated stage kept at 37 °C. Following permeabilization with digitonin, leucine at a final concentration of 1 mM was added. Following 5 minutes of pre-incubation with 1 mM leucine, Ca^{2+} or PAO were added at final concentrations of 250 μM and 5 μM, respectively. Time-lapse microscopy was conducted over a 20 minute time course with TMRM fluorescence intensity assessed as described in Materials and methods. The results are the mean of three independent experiments ± the standard deviation. E and F. HeLa cells were plated at 50,000 cells/well in 24 well plates and transfected with the indicated siRNA. After 48 hours, the cells were loaded with 200 nM TMRM in DMEM for 30 minutes. The cells were incubated further for 5 minutes in respiratory buffer containing 2.5 μg/ml digitonin and 20 nM of TMRM. Fluorescence intensity was measured using a Synergy HT microplate reader with an excitation of 550 nm and emission at 573 nm at 37 °C at 1 minute intervals. After 4 minutes, either phenylarsine oxide or Ca^{2+} was added at the indicated concentrations, with fluorescence measured over 20 minutes. The results are presented as % of TMRM retained in non-treated cells transfected with non target siRNA at the 20 minute time point. The results are the mean of three independent experiments ± the standard deviation.

3.5. Role of mitochondrial glutathione in sirt-4 protection

A stimulation of GDH-1 activity can increase synthesis of NADPH, which in turn can be utilized in the production of reduced glutathione (GSH). Glutathione is an antioxidant, suggesting the possibility that depletion of sirt-4 protects against the PTP by promoting the production of GSH. Control cells or cells transfected with non-targeting siRNA displayed mitochondrial GDH-1 activity of 1.86 μmol/min/mg protein). As shown in Fig. 7A, depletion of sirt-4 stimulated mitochondrial GDH-1 activity to 74% above that seen in untreated control cells. Similarly, as expected the addition of leucine also stimulated GDH-1 activity to 79% above control levels. Importantly, stimulation of GDH-1 activity with

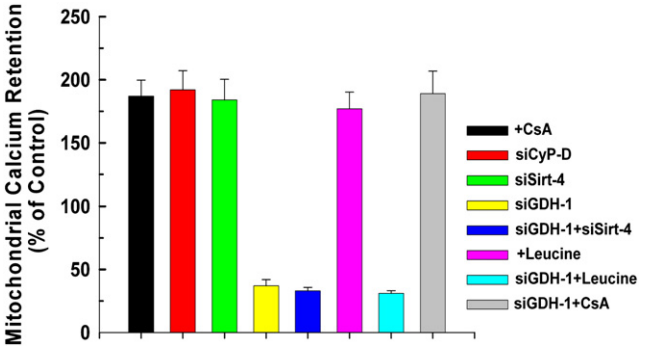

Fig. 6. Depletion of Sirt-4 enhances mitochondrial calcium retention capacity. HeLa cells were plated at 50,000 cells/well in 24 well plates and transfected with the indicated siRNA. After 48 hours, the cells were incubated for 5 minutes in respiratory buffer containing 2.5 μg/ml digitonin and 1 μM of the Ca^{2+} indicator, Calcium Green-5N (excitation 505 nm; emission: 535 nm; Molecular Probes). Calcium was added in pulses of 10 μM and uptake measured as a decrease of Calcium Green-5N fluorescence. The results are the mean of three independent experiments ± the standard deviation.

leucine or by suppression of sirt-4 expression, were both prevented by transfection with siRNA targeting GDH-1. However, despite activating GDH-1, neither depletion of sirt-4 nor the addition of leucine caused an elevation of mitochondrial GSH levels. The concentration of glutathione in mitochondria isolated from control non-treated cells was 6 nmole/mg mitochondrial protein. The concentration of GSSG was 0.3 nmole/mg mitochondrial protein. As shown in Fig. 7B, depletion of sirt-4 or stimulation with leucine did not bring about any appreciable change in the mitochondrial reduced or oxidized glutathione concentration. Surprisingly, depletion of GDH-1 did not provoke a decline of mitochondrial GSH. However, the addition of Ca^{2+} did promote a depletion of mitochondrial GSH and increase of GSSG. However, this is most likely due to opening of the PTP and subsequent loss of GSH, as the Ca^{2+} induced depletion of GSH is prevented by suppression of CyP-D expression or treatment with CsA. Similarly, suppression of sirt-4 expression also prevented the Ca^{2+} induced loss of mitochondrial GSH and increase of GSSG, as did stimulation of GDH-1 activity with leucine. Importantly stimulation of GDH-1 activity by depletion of sirt-4 or addition of leucine did not increase or decrease the GSH/GSSG ratio (Fig. 7C). Together, these data suggest that stimulation of GDH-1 does not cause an absolute increase of mitochondrial GSH levels and the ability of GDH-1 stimulation to prevent onset of the PTP cannot be accounted for solely by modulation of mitochondrial GSH levels.

3.6. Sirt-4 mediates PTP dependent cytotoxicity

We and others have previously demonstrated that TNF induced necroptosis is dependent on PTP induction [18–20]. As shown in Fig. 8A, in L929 fibrosarcoma cells, TNF in the presence of the pan-caspase inhibitor, ZVAD-FMK, induces a massive loss of cell viability, with only 8% of cells transfected with non-target siRNA remaining viable after 24 hours of exposure (black bar). Suppression of CyP-D expression blunted TNF + ZVAD induced cytotoxicity, with 68% of the cells still viable after 24 hours of exposure, demonstrating that in this instance, TNF induced cytotoxicity is PTP dependent (Fig. 8A, red bar). Markedly, suppression of sirt-4 expression also prevented TNF + ZVAD induced cytotoxicity, with 70% of the cells still viable after 24 hours of exposure (Fig. 8A, green bar). By contrast, suppression of sirt-3 or sirt-5 exhibited no ability to prevent TNF + ZVAD induced cell killing (results not shown). Importantly, the ability of sirt-4 down-regulation to inhibit TNF + ZVAD induced cytotoxicity was dependent on GDH-1 expression. As show in Fig. 8A, depletion of GDH-1 reversed the protective effect afforded by sirt-4 down-regulation against TNF + ZVAD induced cytotoxicity, with less than 10% of the cells remaining viable after 24 hours of exposure (yellow bar). Importantly, as with PTP induction in mitochondria, depletion of GDH-1 had no effect on the ability of CyP-D suppression to protect against TNF + ZVAD induced cytotoxicity, with 67% of the cells still viable after 24 hours of exposure (Fig. 8A, blue bar).

Doxorubicin induced cytotoxicity is also dependent on PTP induction [21–23]. As shown in Fig. 8B, doxorubicin at a dose of 50 μM left only 14% of HeLa cells transfected with non-targeting siRNA viable following 18 hours of treatment (black bar). By contrast, suppression of CyP-D or sirt-4 largely prevented doxorubicin induced cytotoxicity, with greater than 70% of the cells still viable following 18 hours of treatment. (Fig. 8B, red and green bars, respectively). Moreover, as with TNF + ZVAD, the protection afforded against doxorubicin induced cytotoxicity brought about by suppressing sirt-4 expression was dependent on GDH-1. As shown in Fig. 6B, depletion of GDH-1 reversed the protective effect of sirt-4 suppression, with only 14% of the cells remaining viable after 18 hours of doxorubicin treatment (yellow bar). By contrast, depletion of GDH-1 did not reverse the protective effect exerted by knock-down of CyP-D, with cell viability maintained at 75% following 18 hours of treatment with doxorubicin (Fig. 8B, blue bar), indicating that the protective effect exerted by down-regulating sirt-4 is dependent on GDH-1, whereas the protection afford by CyP-D suppression is not.

4. Discussion

The present study demonstrates that sirt-4 modulates sensitivity to PTP induction and that this may be mediated partly through regulation of glutamate dehydrogenase-1. Depletion of sirt-4 prevented PTP induction brought about by Ca^{2+} or PAO. Additionally, sirt-4 expression mediated sensitivity to PTP dependent cell death, with suppression of sirt-4 levels preventing TNF + ZVAD and doxorubicin induced cytotoxicity. Importantly, inhibition of PTP sensitivity by down-regulation of sirt-4 is dependent on GDH-1 expression. Depletion of GDH-1 negated the protective effect exerted by suppressing sirt-4 levels against PTP induction brought about by Ca^{2+} and PAO, and also prevented sirt-4 suppression from inhibiting TNF + ZVAD or doxorubicin induced cytotoxicity. By contrast, suppression of PTP induction or inhibition of PTP dependent cytotoxicity by down-regulating CyP-D was insensitive to GDH-1 levels. Moreover, pre-treatment with the GDH-1 allosteric activator, leucine, prevented PTP induction, with depletion of GDH-1 reversing the protective effect of leucine. These data suggest that by negatively regulating GDH-1, sirt-4 increases sensitivity to PTP induction and that when sirt-4 levels are suppressed, activation of GDH-1 promotes resistance to PTP induction and subsequent cytotoxicity.

The regulation of GDH-1 activity by ADP-ribosylation was noted before the identification of sirt-4 as the enzyme responsible for the modification [24,25]. GDH-1 is active as a homohexamer, but the stoichiometry between incorporated ADP-ribose and GDH-1 subunits indicates that ADP-ribosylation of one subunit of the hexameric complex maybe all that is needed for its inactivation [26]. The cysteine residue at position 119 is the site ADP-ribosylated by sirt-4, but curiously is thought not to be directly involved in GDH-1 catalysis, as cysteine residue 323 has been shown to be. In addition to ADP-ribosylation, GDH-1 is controlled by a number of allosteric effectors including ADP, ATP, GDP, GTP and leucine [16,17].

Sirt-4 is localized to the mitochondrial matrix but possesses no deacetylase activity. Rather, sirt-4 ADP-ribosylates GDH-1, thereby inhibiting its activity and provoking a number of metabolic alterations [14]. In pancreatic β cells, suppression of sirt-4 resulted in activation of GDH-1 that in turn provoked an increase in insulin secretion in response to glucose [15]. The ability of GDH-1 to promote insulin secretion was also identified in dominant mutations of GDH-1 that cause reduced GTP inhibition of the enzyme, resulting in a

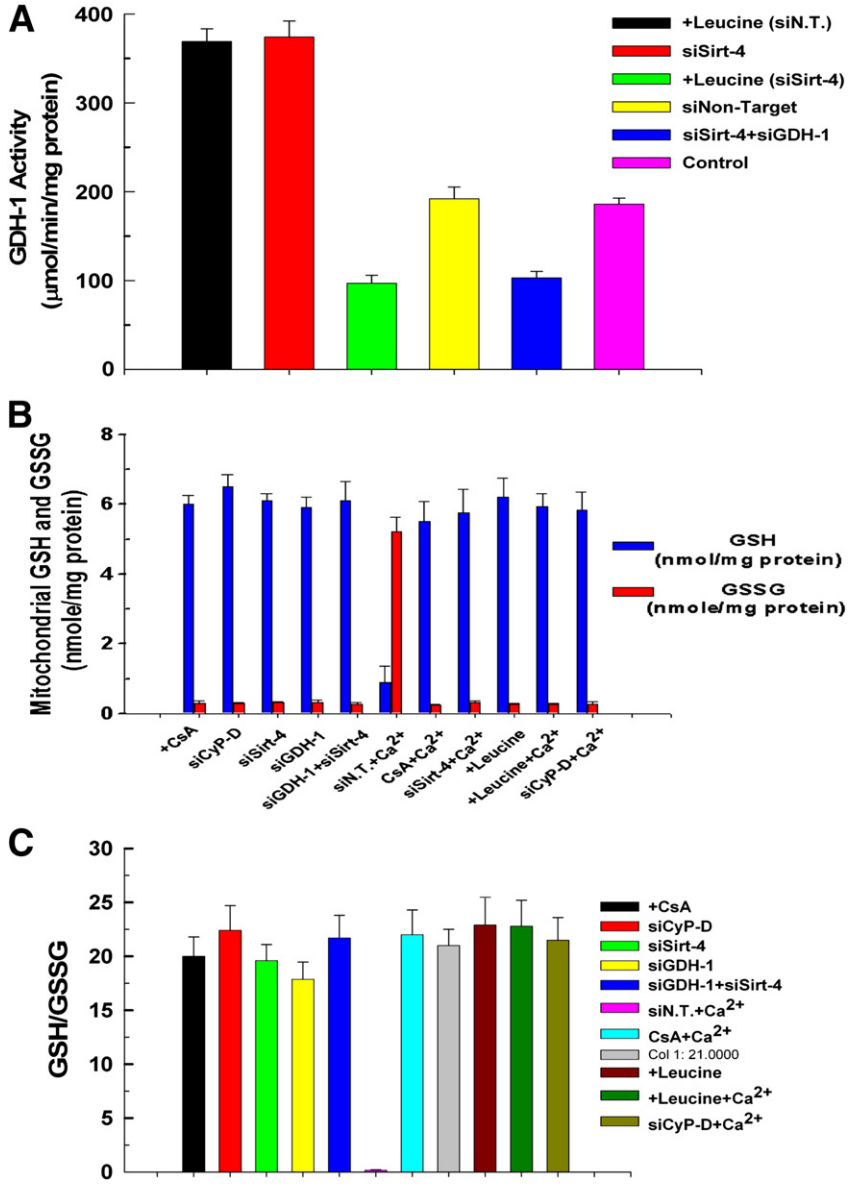

Fig. 7. GDH-1 activity and mitochondrial GSH. A. HeLa cells were plated at 50,000 cells/well in 24 well plates and transfected with the indicated siRNA. Forty eight hours after transfection, cells from 4 wells were harvested by trypsinization and washed twice with ice cold PBS. Mitochondria were isolated and lysates prepared. Optical density at 450 nm was measured with Synergy HT microplate reader (BioTek, Winooski, VT) at 37 °C at 3 minute intervals for 1 hour. The results are expressed in percentage increase or decrease in activity compared to non-treated cells transfected with non-targeting control siRNA. The results are the mean of three independent experiments ± the standard deviation. B. HeLa cells were plated at 50,000 cells/well in 24 well plates and transfected with the indicated siRNA. Forty eight hours after transfection, cells from 4 wells were harvested by trypsinization and washed twice with ice cold PBS. Mitochondria were isolated and lysates prepared. The supernatant was used to determine the GSH content. Fluorescence was measured at excitation of 308 nm and emission of 460 nm using a Synergy HT microplate reader. The results are presented as percentage of GSH content compared to non-treated and non-target transfected cells. The results are the mean of three independent experiments ± the standard deviation. C. The GSH/GSSG ratio was calculated from the measured concentrations of GSH and GSSG.

syndrome of hyperinsulinism and hyperammonemia [27]. Sirt-4 has also been shown to interact with insulin degrading enzyme (IDE) and adenine nucleotide translocase 2 (ANT-2). ANT-2 mediates the uptake of ATP from the cytosol into the mitochondria and exhibits increased expression in highly glycolytic cancer cells [28,29]. Expression of ANT-2 is associated with inhibition of apoptosis, although the exact mechanism by which it exerts this effect is unclear. However down-regulating ANT-2 or IDE had no effect on the ability of sirt-4 to modulate sensitivity to PTP induction (results not shown). Intriguingly, mutations of the pancreatic duodenal homeobox gene-1 (Pdx-1) cause heritable diabetes in humans and mice, brought about by increased pancreatic beta cell death mediated by onset of the PTP, suggesting that in pancreatic beta cells, sirt-4 may contribute to regulation of the PTP [30,31].

The mechanism by which suppression of sirt-4 inhibits PTP induction is unclear. The dependence on GDH-1 expression may indicate that it involves metabolic alterations in mitochondrial metabolism. In an anapleurotic reaction, increased GDH-1 activity funnels glutamate into the tricarboxylic acid cycle via α-ketoglutarate dehydrogenase, resulting in an elevation of NADPH, NADH and ATP production; all of which increase the threshold for PTP induction. [26] Alternatively, once activated, GDH-1 in its hexameric configuration may interact with a component of the PTP to inhibit assembly of the pore complex. Interestingly, before the concept of a permeability transition pore emerged, it was shown that ADP-ribosylation controlled sensitivity to the mitochondrial permeability transition [32–35]. Mono-ADP-ribosylation of mitochondrial proteins is stimulated by pro-oxidants and is associated with loss of mitochondrial membrane integrity. It is possible that the ADP-ribosyltransferase

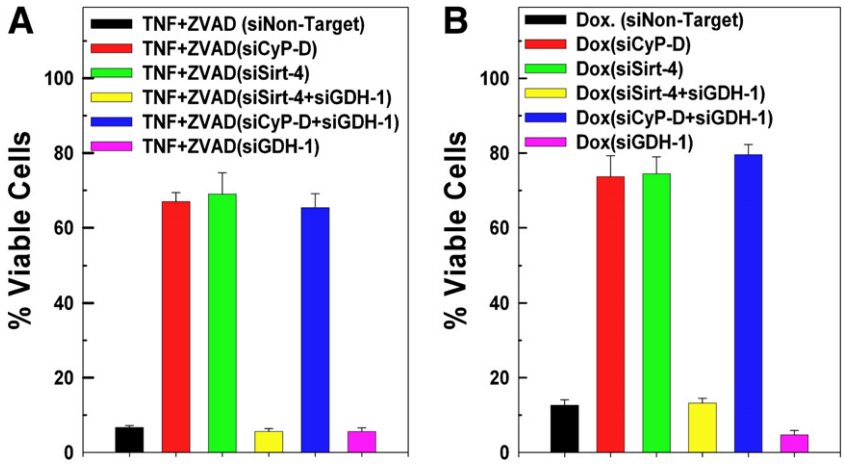

Fig. 8. Down-regulation of sirt-4 prevents TNF and doxorubicin cytotoxicity. A and B. HeLa cells were transfected with 50 nM of a non-targeting control siRNA or siRNAs targeting sirt-4 or CyP-D, separately or in tandem with siRNA targeting GDH-1 or siGDH-1 alone. Following 48 hours incubation, the cells were incubated with 20 ng/ml of TNFα in the presence of 20 μM of ZVAD, or treated with 10 μM of doxorubicin. After 24 hours, the cells were harvested and cell viability assessed utilizing propidium iodide as described in Materials and methods. Values are the means of three independent experiments with the error bars indicating standard deviations.

activity responsible for this phenomenon is partly mediated by sirt-4. Indeed, it maybe that sirt-4 ADP-ribosylates and modulates multiple targets that impact sensitivity to PTP induction.

In summary, the present study provides evidence indicating that sirt-4 modulates sensitivity to mitochondrial PTP induction and PTP dependent cytotoxicity that is in part dependent on GDH-1 (Fig. 9).

Acknowledgements

This work was supported in part from grants from the National Cancer Institute and the National Institute of Alcohol Abuse and Alcoholism.

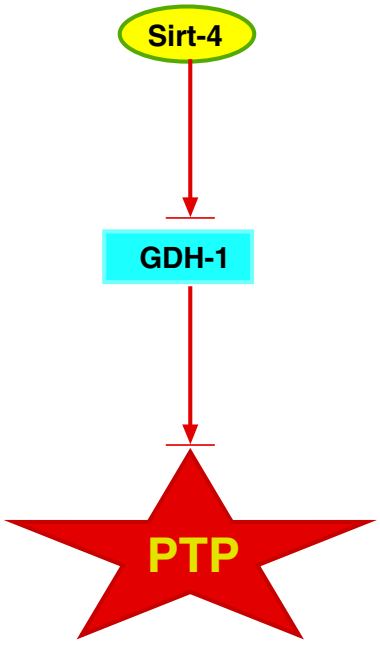

Fig. 9. Control of mitochondrial permeability transition pore sensitivity by Sirt-4. Proposed pathway by which modulation of sirt-4 activity can stimulate GDH-1, which in turn inhibits PTP opening and loss of cell viability.

References

[1] F. Di Lisa, R. Menabo, M. Canton, M. Barile, P. Bernardi, Opening of the mitochondrial permeability transition pore causes depletion of mitochondrial and cytosolic NAD+ and is a causative event in the death of myocytes in postischemic reperfusion of the heart, J. Biol. Chem. 276 (2001) 2571–2575.
[2] A.P. Halestrap, C.P. Connern, E.J. Griffiths, P.M. Kerr, Cyclosporin A binding to mitochondrial cyclophilin inhibits the permeability transition pore and protects hearts from ischaemia/reperfusion injury, Mol. Cell. Biochem. 174 (1997) 167–172.
[3] V.G. Sharov, A. Todor, S. Khanal, M. Imai, H.N. Sabbah, Cyclosporine A attenuates mitochondrial permeability transition and improves mitochondrial respiratory function in cardiomyocytes isolated from dogs with heart failure, J. Mol. Cell. Cardiol. 42 (2007) 150–158.
[4] C.P. Baines, R.A. Kaiser, N.H. Purcell, N.S. Blair, H. Osinska, M.A. Hambleton, E.W. Brunskill, M.R. Sayen, R.A. Gottlieb, G.W. Dorn, J. Robbins, J.D. Molkentin, Loss of cyclophilin D reveals a critical role for mitochondrial permeability transition in cell death, Nature 434 (2005) 658–662.
[5] T. Nakagawa, S. Shimizu, T. Watanabe, O. Yamaguchi, K. Otsu, H. Yamagata, H. Inohara, T. Kubo, Y. Tsujimoto, Cyclophilin D-dependent mitochondrial permeability transition regulates some necrotic but not apoptotic cell death, Nature 434 (2005) 652–658.
[6] I. Szabo, P. Bernardi, M. Zoratti, Modulation of the mitochondrial megachannel by divalent cations and protons, J. Biol. Chem. 267 (1992) 2940–2946.
[7] P. Bernardi, Modulation of the mitochondrial cyclosporin A-sensitive permeability transition pore by the proton electrochemical gradient. Evidence that the pore can be opened by membrane depolarization, J. Biol. Chem. 267 (1992) 8834–8839.
[8] P. Bernardi, S. Vassanelli, P. Veronese, R. Colonna, I. Szabo, M. Zoratti, Modulation of the mitochondrial permeability transition pore. Effect of protons and divalent cations, J. Biol. Chem. 267 (1992) 2934–2939.
[9] E. Lenartowicz, P. Bernardi, G.F. Azzone, Phenylarsine oxide induces the cyclosporin A-sensitive membrane permeability transition in rat liver mitochondria, J. Bioenerg. Biomembr. 23 (1991) 679–688.
[10] P. Korge, J.I. Goldhaber, J.N. Weiss, Phenylarsine oxide induces mitochondrial permeability transition, hypercontracture, and cardiac cell death, Am. J. Physiol. Heart Circ. Physiol. 280 (2001) H2203–H2213.
[11] B.H. Ahn, H.S. Kim, S. Song, I.H. Lee, J. Liu, A. Vassilopoulos, C.X. Deng, T. Finkel, A role for the mitochondrial deacetylase Sirt3 in regulating energy homeostasis, Proc. Natl. Acad. Sci. U. S. A. 105 (2008) 14447–14452.
[12] T. Nakagawa, D.J. Lomb, M.C. Haigis, L. Guarente, SIRT5 deacetylates carbamoyl phosphate synthetase 1 and regulates the urea cycle, Cell 137 (2009) 560–570.
[13] N. Shulga, R. Wilson-Smith, J.G. Pastorino, Sirtuin-3 deacetylation of cyclophilin D induces dissociation of hexokinase II from the mitochondria, J. Cell Sci. 123 (2010) 894–902.
[14] M.C. Haigis, R. Mostoslavsky, K.M. Haigis, K. Fahie, D.C. Christodoulou, A.J. Murphy, D.M. Valenzuela, G.D. Yancopoulos, M. Karow, G. Blander, C. Wolberger, T.A. Prolla, R. Weindruch, F.W. Alt, L. Guarente, SIRT4 inhibits glutamate dehydrogenase and opposes the effects of calorie restriction in pancreatic beta cells, Cell 126 (2006) 941–954.
[15] N. Ahuja, B. Schwer, S. Carobbio, D. Waltregny, B.J. North, V. Castronovo, P. Maechler, E. Verdin, Regulation of insulin secretion by SIRT4, a mitochondrial ADP-ribosyltransferase, J. Biol. Chem. 282 (2007) 33583–33592.
[16] T. Tomita, T. Kuzuyama, M. Nishiyama, Structural basis for leucine-induced allosteric activation of glutamate dehydrogenase, J. Biol. Chem. 286 (2011) 37406–37413.

[17] M. Li, C. Li, A. Allen, C.A. Stanley, T.J. Smith, The structure and allosteric regulation of mammalian glutamate dehydrogenase, Arch. Biochem. Biophys. 519 (2011) 69–80.
[18] J.G. Pastorino, G. Simbula, K. Yamamoto, P.A. Glascott Jr., R.J. Rothman, J.L. Farber, The cytotoxicity of tumor necrosis factor depends on induction of the mitochondrial permeability transition, J. Biol. Chem. 271 (1996) 29792–29798.
[19] C.A. Bradham, T. Qian, K. Streetz, C. Trautwein, D.A. Brenner, J.J. Lemasters, The mitochondrial permeability transition is required for tumor necrosis factor alpha-mediated apoptosis and cytochrome c release, Mol. Cell. Biol. 18 (1998) 6353–6364.
[20] C. Garcia-Ruiz, A. Colell, A. Morales, M. Calvo, C. Enrich, J.C. Fernandez-Checa, Trafficking of ganglioside GD3 to mitochondria by tumor necrosis factor-alpha, J. Biol. Chem. 277 (2002) 36443–36448.
[21] D. Montaigne, X. Marechal, S. Preau, R. Baccouch, T. Modine, G. Fayad, S. Lancel, R. Neviere, Doxorubicin induces mitochondrial permeability transition and contractile dysfunction in the human myocardium, Mitochondrion 11 (2010) 22–26.
[22] S. Zhou, A. Starkov, M.K. Froberg, R.L. Leino, K.B. Wallace, Cumulative and irreversible cardiac mitochondrial dysfunction induced by doxorubicin, Cancer Res. 61 (2001) 771–777.
[23] S. Cardoso, R.X. Santos, C. Carvalho, S. Correia, G.C. Pereira, S.S. Pereira, P.J. Oliveira, M.S. Santos, T. Proenca, P.I. Moreira, Doxorubicin increases the susceptibility of brain mitochondria to Ca(2+)-induced permeability transition and oxidative damage, Free Radic. Biol. Med. 45 (2008) 1395–1402.
[24] M.M. Choi, J.W. Huh, S.J. Yang, E.H. Cho, S.Y. Choi, S.W. Cho, Identification of ADP-ribosylation site in human glutamate dehydrogenase isozymes, FEBS Lett. 579 (2005) 4125–4130.
[25] A. Herrero-Yraola, S.M. Bakhit, P. Franke, C. Weise, M. Schweiger, D. Jorcke, M. Ziegler, Regulation of glutamate dehydrogenase by reversible ADP-ribosylation in mitochondria, EMBO J. 20 (2001) 2404–2412.
[26] M. Karaca, F. Frigerio, P. Maechler, From pancreatic islets to central nervous system, the importance of glutamate dehydrogenase for the control of energy homeostasis, Neurochem. Int. 59 (2011) 510–517.
[27] R.R. Kapoor, S.E. Flanagan, P. Fulton, A. Chakrapani, B. Chadefaux, T. Ben-Omran, I. Banerjee, J.P. Shield, S. Ellard, K. Hussain, Hyperinsulinism-hyperammonaemia syndrome: novel mutations in the GLUD1 gene and genotype-phenotype correlations, Eur. J. Endocrinol. 161 (2009) 731–735.
[28] A. Chevrollier, D. Loiseau, P. Reynier, G. Stepien, Adenine nucleotide translocase 2 is a key mitochondrial protein in cancer metabolism, Biochim. Biophys. Acta 1807 (2010) 562–567.
[29] A. Chevrollier, D. Loiseau, B. Chabi, G. Renier, O. Douay, Y. Malthiery, G. Stepien, ANT2 isoform required for cancer cell glycolysis, J. Bioenerg. Biomembr. 37 (2005) 307–316.
[30] K. Fujimoto, E.L. Ford, H. Tran, B.M. Wice, S.D. Crosby, G.W. Dorn 2nd, K.S. Polonsky, Loss of Nix in Pdx1-deficient mice prevents apoptotic and necrotic beta cell death and diabetes, J. Clin. Invest. 120 (2010) 4031–4039.
[31] K. Fujimoto, Y. Chen, K.S. Polonsky, G.W. Dorn II, Targeting cyclophilin D and the mitochondrial permeability transition enhances beta-cell survival and prevents diabetes in Pdx1 deficiency, Proc. Natl. Acad. Sci. U. S. A. 107 (2010) 10214–10219.
[32] A. Masmoudi, F. Islam, P. Mandel, ADP-ribosylation of highly purified rat brain mitochondria, J. Neurochem. 51 (1988) 188–193.
[33] B. Frei, C. Richter, Mono(ADP-ribosylation) in rat liver mitochondria, Biochemistry 27 (1988) 529–535.
[34] C. Richter, B. Frei, Ca2+ release from mitochondria induced by prooxidants, Free Radic. Biol. Med. 4 (1988) 365–375.
[35] C. Richter, K.H. Winterhalter, S. Baumhuter, H.R. Lotscher, B. Moser, ADP-ribosylation in inner membrane of rat liver mitochondria, Proc. Natl. Acad. Sci. U. S. A. 80 (1983) 3188–3192.